ELSEVIER

Catalysis Today 57 (2000) 193–199

CATALYSIS TODAY

www.elsevier.com/locate/cattod

Preparation, characterization and catalytic properties of $Co–Nb_2O_5–SiO_2$ catalysts

V. Pârvulescu [a], V.I. Pârvulescu [b,*], P. Grange [c]

[a] *Institute of Physical Chemistry, Splaiul Independentei 202, Bucharest 77208, Romania*
[b] *Department of Chemical Technology and Catalysis, Faculty of Chemistry, University of Bucharest, B-dul Regina Elisabeta 4-12, Bucharest 70346, Romania*
[c] *Université catholique de Louvain, Unité de Catalyse et chimie des matériaux divisés, Place Croix du Sud 2, bte 17, 1348 Louvain-la-Neuve, Belgium*

Abstract

$Co–Nb_2O_5–SiO_2$ catalysts were prepared using three different sol–gel procedures: (i) the colloidal sol–gel method using $NbCl_5$ and $SiCl_4$ as precursors; (ii) the polymeric sol–gel method using niobium ethoxide and tetraethyl-orthosilicate (TEOS); (iii) an intermediate procedure between the colloidal and polymeric sol–gel method in which the precursors were those utilized in the CSG but dissolved in a mixture of anhydrous ethanol and CCl_4. In all procedures, the elimination of the solvent carried out between 80 and 110°C was followed by a reduction in hydrogen flow (30 ml min^{-1}) at 773 K. Following these procedures, samples containing 10 wt.% Co and 15 wt.% niobium oxide (expressed as Nb_2O_5) were obtained. The characterization of the catalysts was performed using various techniques: N_2 adsorption and desorption curves at 77 K, NH_3- and H_2-chemisorption, TPO, XPS, XRD, and solid state ^1H MAS-NMR. Hydrogenolysis of butane was evaluated. The low reaction rates are assigned to the effect of the metal size, whereas the isobutane selectivity as well as the relatively high stability is due to the acidity of the support.

Keywords: $Co–Nb_2O_5–SiO_2$ catalysts; Sol–gel technique; NH_3- and H_2-chemisorption; TPO; XPS; XRD; Solid state ^1H MAS-NMR; Butane hydrogenolysis

1. Introduction

The investigation of niobium containing catalysts received an increased interest since it was shown that the materials containing this element could be very useful promoters, catalyst supports or even catalysts for the reactions of practical importance [1]. The acidic and redox properties of these solids mainly determined this interest. Most of the transition metal–supported catalysts containing niobia as support or promoter are bifunctional, i.e. strong acid sites coexist with metallic species on the same catalyst. Redox properties are a key factor in the development of SMSI for metal catalysts subjected to a high temperature reduction [2]. In addition, the possibility to obtain mesoporous niobia supports made this element even more attractive.

Among the various methods of preparation, the use of the sol–gel procedures was intensively reported [3,4]. High surface area niobia with a relatively large pore size distribution were obtained in this way. The thermal stability of niobia aerogels prepared using sol–gel is relatively low and crystallization producing a loss of the strongest acid sites is observed after heating at 873 K. High surface areas and thermally stable support could be obtained by careful dispersion of the niobia in a solid matrix. In this regard silica is a

* Corresponding author.

0920-5861/00/$ – see front matter
PII: S0920-5861(99)00326-0

particular good choice: silica obtained by sol–gel method has a very high surface area. In addition silica and niobia have a complete immiscibility in all compositions in range [5]. According to Tanabe [6] niobia–silica mixed oxide will exhibit an increased acidity caused by the imbalance charge along Si–O–Nb linkages. The studies reported in the last decade on the catalytic behavior of this mixed oxide account to these characteristics [7–10].

In a previous study on cobalt–niobia catalysts we reported that the colloidal sol–gel technique also offers a tool to control both the structure and the homogeneity of the system [11]. The appearance of the SMSI effect was evidenced after reduction by hydrogen at temperatures higher than 823 K.

The aim of this study was to prepare bifunctional $Co–Nb_2O_5–SiO_2$ catalysts in a one-step procedure using the sol–gel technique.

2. Experimental

The preparation of niobia–silica catalysts was made using various procedures: (i) The colloidal sol–gel method (CSG) using $NbCl_5$ and $SiCl_4$ as precursors. Colloidal suspensions of niobium hydroxide and silica in anhydrous ethanol were independently obtained by precipitation of $NbCl_5$, and $SiCl_4$ with Na_2CO_3 solution or H_2O, respectively. In this way, precipitates exhibiting various colloid sizes were obtained and peptized in acid conditions (HCl). The aqueous $Co(NO_3)_2$ solution was added to the resulting colloidal suspensions. The gelation process was carried out at 333 K for 7 days. These samples are denoted by A. (ii) The polymeric sol–gel method (PSG) used niobium ethoxide as niobium source, and tetraethyl-orthosilicate (TEOS), as silicon one. The hydrolysis of TEOS dissolved in ethanol has been carried out at a water:TEOS molar ratio of 1:5 at acid pH (HCl), under reflux conditions. The niobium ethoxide solution was added after 2 h and then $Co(NO_3)_2$ in ethanol was added. The gelation process was carried out under vigorous stirring at room temperature for 8 h. These samples are denoted by B. (iii) An intermediate procedure between the colloidal and polymeric sol–gel method in which the precursors were those utilized in the CSG but dissolved in a mixture of anhydrous ethanol with CCl_4 was also used. Partial hydrolysis of the salts and the gelation process were carried out at acid pH (HCl) in the presence of traces of H_2O remaining in the alcoholic phase. The distribution of cobalt and the porous structure were controlled by adding together the alcoholic solution, $Co(NO_3)_2$, and a templating agent (PEG's 2000). These samples are denoted by C. In all procedures, the elimination of the solvent was carried out in the 353–383 K range followed by reduction at 773 K, under hydrogen flow (30 ml min^{-1}). Following these procedures, samples containing 10 wt.% Co and 15 wt.% niobium oxide (expressed as Nb_2O_5) were obtained. The chemical composition and the textural characteristics are given in Table 1.

The characterization of the catalysts was performed using various techniques: N_2 adsorption and desorption at 77 K, NH_3 and H_2-chemisorption, XPS, XRD and solid state ^1H MAS-NMR.

NH_3 and H_2-chemisorption were carried out using a Micromeritics ASAP 2010 C. For H_2-chemisorption, the reduced samples were evacuated, first at 393 K and then at 723 K. Soon after, a hydrogen flow was passed initially at 308 K for 15 min and then temperature was increased at 723 K at a heating rate of 10 K min^{-1} and maintained at this temperature for 2 h. After reduction, the samples were purged with a helium flow at 690 K for 2 h and then at 308 K for another 30 min. The amount of chemisorbed hydrogen were measured at 308 K after equilibration for 45 min in 300 Torr of adsorbate. The total hydrogen uptake was determined by extrapolating the linear portion of the adsorption isotherm to zero pressure. Reversible H_2 sorption was measured by out gassing at 5×10^{-5} Torr

Table 1
Chemical composition and textural properties of the catalysts

Catalyst	Cobalt content (wt.%)	Niobia content (wt.%)	BET surface area ($m^2\,g^{-1}$)	Mean pore diameter (nm)
Sample A	9.96	14.85	96	2.1
Sample B	9.93	14.92	180	2.0
Sample C	10.12	14.78	105	3.2

at the adsorption temperature and running a second isotherm. The difference between the total and reversible uptakes was ascribed to irreversible hydrogen. The cobalt dispersion was determined from the irreversible uptake, assuming a H:Co stoichiometry of 1 [12]. H_2-chemisorption data considered the reduced Co species to be those which were determined in conditions of temperature-programmed oxidation (TPO) experiments. These experiments were performed using a Micromeritics Pulse Chemisorb 2705 apparatus at a 50 ml min^{-1} O_2 (5%)–He flow. Reduced cobalt was determined assuming that at 773 K all Co was converted to Co_3O_4. This assumption was confirmed also by XRD and XPS. The actual fraction of Co was used to determine the metal dispersion. Temperature-programmed reduction (TPR) was carried out in the same set-up as that used for TPO experiments. For NH_3-chemisorption the evacuated samples were subjected to analysis first at 312 K, and then at 473 K. The amount of chemisorbed NH_3 was also determined from the irreversible uptake.

The XPS spectra were recorded using a SSI X probe FISONS spectrometer (SSX-100/206) with monochromated Al Kα radiation. The spectrometer energy scale was calibrated using the $Au4f_{7/2}$ peak (binding energy 84.0 eV). For calculation of the binding energies, the C_{1s} peak of the C–(C,H) component of adventitious carbon at 284.8 eV was used as an internal standard. The composite peaks were decomposed by a fitting routine included in the ESCA 8,3 D software. The bands assigned to Co_{3p}, Nb_{3d}, Si_{2p}, and O_{1s} were analysed.

XRD patterns were recorded with a SIEMENS D-5000 diffractometer operating at 40 kV and 50 mA. The diffractograms were recorded between 2 and 80° 2θ at a scanning speed of 0.5 2θ min^{-1}, using Cu Kα radiation (λ=1.5418 Å).

Solid state ^{1}H MAS-NMR spectra were obtained at room temperature using a Varian VXR-400S spectrometer with an Oxford cryomagnet, operated at a Sun workstation network with a V NMR operating system version 4.1. The Fourier transform of free induction decay (FID) was observed using a quadrature detection at a spinning rate of 6000 rot min^{-1} for more than 2 h acquisition time. About 0.5 g catalyst powder, outgassed by heating at 125°C, was introduced into the spectrometer sample holder and tuned at the minimum signal possible for proton analysis. The chemical shift of the peaks observed from the spectra were corrected using the same reference for each sample (−133 ppm).

Butane hydrogenolysis was carried out in a quartz microreactor connected on-line to a Hewlett-Packard 5890 Series II Gas Chromatograph. The reactants and products were separated on a 6 m column containing Chromosorb W coated with silicon oil. The experiments were carried out at 473 K. The alkane flow was kept constant at 30 ml min^{-1}. Hydrogen was purified through a Deoxo catalytic purifier and two traps (silica gel and zeolite 13X). Butane purity was higher than 99.95%. Before reaction, butane was passed through a trap containing zeolite 4A. In these conditions, the conversions were below 15%. The evolution of the reaction was followed by the decrease of the concentration of the reactant expressed as a percentage of the total carbon. Each experiment used 0.3 g catalyst. The reaction rates were expressed as a mmole alkane reacted, g_{Co}^{-1} h^{-1}. The selectivity of product j was defined using Bond's formula [13,14]: $S_j = c_j/A$, where c_j is the molar fraction of products containing j carbon atoms ($j<4$), and A is the number of moles converted. The isomerization selectivity (Si) is the fraction of butane converted to isobutane. Data were recorded after 5 min of reaction. Long-run experiments allow to evaluate the stability of the catalysts.

3. Results

3.1. Acidity of the catalysts

3.1.1. NH_3 chemisorption

Fig. 1 shows the variation of the acidity of the catalysts. Both at 312 K and at 473 K, sample B exhibits the highest acidity. The measurements performed at

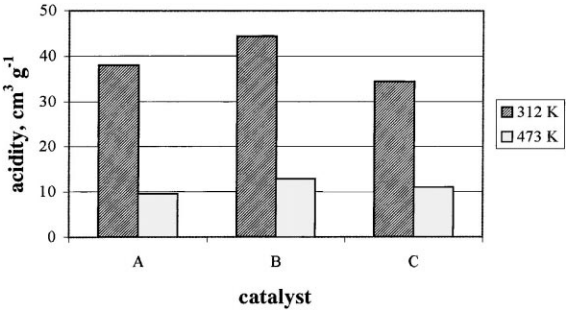

Fig. 1. Variation of the acidity of the catalysts.

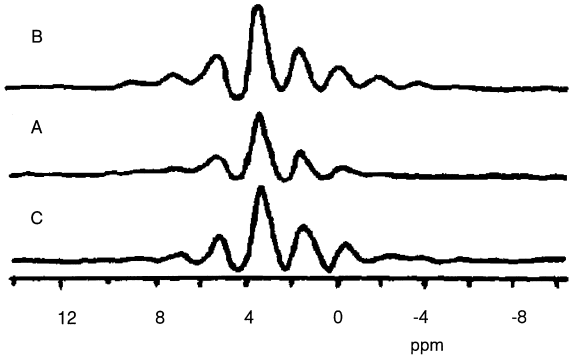

Fig. 2. ^{1}H NMR spectra of the samples.

473 K indicate an important decrease of the acidity (more than 60%) as compared with those obtained at 312 K. At such low temperature, the differences between the various samples become almost insignificant. However, at this temperature the lowest acidity was determined for sample A.

3.1.2. Solid state ^{1}H MAS-NMR

The ^{1}H MAS-NMR spectra obtained for the samples prepared via different procedures are presented in Fig. 2. The NMR spectra shows specific signals of protons of various configurations. However, the origin of these signals is difficult to explain by the analysis of chemical shift and the corresponding structural information. Taking these limitations into account, the shape of the spectra presented in Fig. 2 indicates, for all the catalyst samples, the co-existence of different proton species exhibiting different chemical shifts.

3.2. H_2 chemisorption

The H_2 chemisorption data and the reduction degrees determined from TPO are given in Table 2. The reduction degrees were rather small for all the catalysts. Sample B exhibits the lower reduction degree.

The introduction of cobalt in the matrix obtained via the polymeric sol–gel method also leads to an increased dispersion of the metal. Taking into account the high metal loading (10 wt.%) quite unexpected high dispersions were obtained. The use of PEG 2000 for sample C leads to a metal dispersion which is slightly higher than that of sample A obtained via the colloidal sol–gel method.

3.3. XRD

Fig. 3 shows the XRD results. This pattern does not detect bulk mixed silica and nobia compounds. Cobalt is present in three different species: Co (ASTM 15-0806), Co_3O_4 (ASTM 9-0418), and $CoNb_2O_6$ (ASTM 32-0304), respectively. In addition, these patterns include peaks corresponding to Nb_2O_5 (ASTM 30-0872) and two different species of silica (ASTM 18-1170 and 39-1425). The modification of the preparation procedure does not modify the phase composition of the samples except in sample B where only one type of silica, namely that corresponding to ASTM 39-1425, was identified. For sample C this phase is also the main one as compared with that corresponding to ASTM 18-1170.

In conclusion, whatever the sol–gel method used in the preparation of these materials, an almost similar phase structure resulted. According to the XRD patterns, part of cobalt and niobium forms a cobalt niobate, but no compound of cobalt or niobium with silicon was identified.

3.4. XPS

XPS results are presented in Table 3. The location of the binding energies corresponds to cobalt in Co_3O_4 and $CoNb_2O_6$ species [14]. No clear differences were found between these samples. That means that the introduction of cobalt in the niobia–silica matrix re-

Table 2
Hydrogen uptake, metal dispersion, metal surface area and crystallite metal size of Co–Nb_2O_5–SiO_2 catalysts

Catalyst	Degree of reduction (%)	H_2 uptake (μmol g_{cat}^{-1})	Cobalt dispersion (%)	Metal surface area ($m^2\,g^{-1}$)
Sample A	7.4	20.4	16.3	0.81
Sample B	5.0	22.6	26.7	0.90
Sample C	6.3	18.7	18.1	0.74

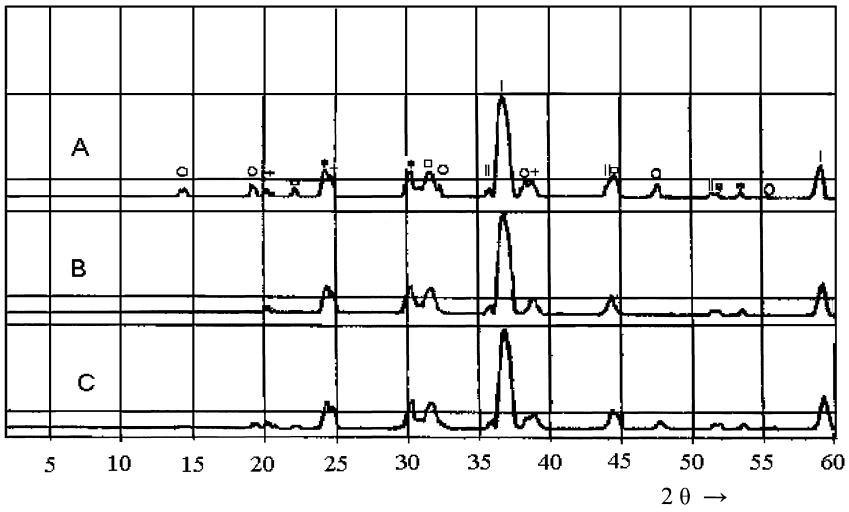

Fig. 3. XRD patterns of the catalysts. (|) Co (ASTM 15-0806), (‖) Co_3O_4 (ASTM 9-0418), (*) $CoNb_2O_6$ (ASTM 32-0304), (+) Nb_2O_5 (ASTM 30-0872), (○) SiO_2 (ASTM 18-1170), and (-) SiO_2 (ASTM 39-1425).

sults in the formation of $CoNb_2O_6$. However, part of cobalt remains as Co_3O_4, and traces of cobalt metal as evidenced by TPO and XRD.

Fig. 4 reports the atomic Co/(Co+Nb+Si) and Nb/(Co+Nb+Si) XPS. The sample obtained using the polymeric sol–gel method shows an increased homogeneity. The positive effect of PEG 2000 in the gelation process results in a more homogeneous distribution both of Co and Nb in sample C as compared with the distribution of the same elements in sample A.

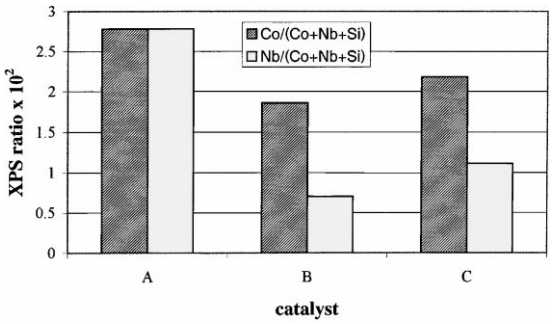

Fig. 4. Surface composition of the catalysts.

3.5. Butane hydrogenolysis

Fig. 5 shows the variation in the reaction rate. Very small differences in the reaction rate with the preparation procedure were determined. Sample B is slightly more active than the others. This behavior can be explained by the very close phase compositions and metal dispersion of these catalysts. In the same time, the values of the reaction rates were relatively low as compared with those reported for the same reaction on other catalysts [15–17].

Table 3
XPS characteristics of the catalysts

Catalyst	Binding energy (eV)					
	Co_3O_4	$Co_2Nb_2O_6$		Nb_2O_5		SiO_2
	$Co_{2p_{3/2}}$	$Co_{2p_{1/2}}$	$Co_{2p_{3/2}}$ (satellite)	$Nb_{3d_{5/2}}$	$Nb_{3d_{3/2}}$	Si_{2p}
Sample A	779.3	781.7	786.8	207.7	210.5	103.3
Sample B	779.2	781.1	786.4	207.2	209.9	103.6
Sample C	779.1	781.5	786.8	207.8	210.7	103.5

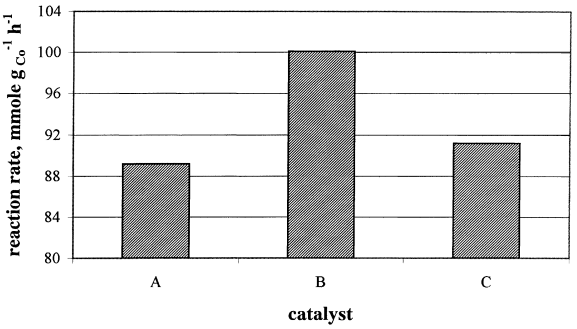

Fig. 5. Butane hydrogenolysis reaction rate.

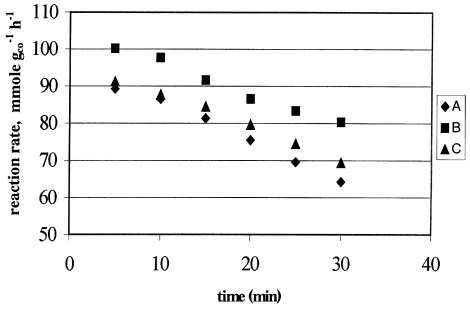

Fig. 7. Evolution of the reaction rate vs time of reaction.

Fig. 6 shows the variation in the selectivity to methane, ethane and isobutane. The selectivities vary in the same sense as the reaction rate. The selectivity towards methane exhibits a maximum for sample B, which presents the highest dispersion of both cobalt and niobium in the silica matrix. The selectivity to isobutane varies with the change of the acidity of these catalysts. One should remark that the conversion of butane to isobutane on these catalysts is about three times higher than that obtained on cobalt–niobia catalysts under similar experimental conditions [11]. This behavior could be a consequence of the higher acidity of niobia–silica matrix.

The decay in the reaction rate after 30 min was $<$28% (Fig. 7).

4. Discussion

The preparation of Co–Nb_2O_5–SiO_2 catalysts containing 10 wt.% Co and 15 wt.% Nb_2O_5 using various sol–gel procedures, introducing cobalt as a $Co(NO_3)_2$ solution in the gelation process of mixed niobia–silica sols, leads to rather homogeneous systems. However, even under such conditions, no mixed compounds containing both niobium and silicon were obtained confirming the fact that the two oxides are immiscible compounds. Also, no mixed compound of cobalt with silicon was observed under such conditions. In all the samples a cobalt niobate phase was obtained. In addition Co_3O_4, reduced Co phases and niobia segregated. Separate silica phases were also identified. The XRD peaks corresponding to silica and niobia (representing 90 wt.% of the catalysts loading) exhibit a small intensity as compared with those of Co_3O_4 which is about 6 wt.% or less. That means that most of silica and niobia form an amorphous structure in which the cobalt-containing species are well dispersed.

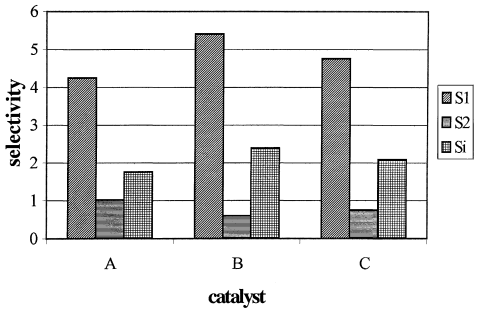

Fig. 6. Variation of the selectivity. (S1) methane; (S2) ethane; (Si) isobutane.

The highest acidity of these catalysts, as compared with that of cobalt–niobia [11], suggests the presence of Si–O–Nb bonds. The use of the polymeric sol–gel procedures allows to increase homogeneity and several characteristics account for such a behavior: the acidity is increased, and the dispersion of cobalt in sample B is higher than with both A and C catalysts.

NH_3-chemisorption carried out at 312 K indicate mainly the existence of Brönsted acidity attributed to the protons located in the close proximity of niobium. The acidity measured at 473 K indicates a partially dehydrated solid surface containing Lewis type sites. It is very probable that these sites are Nb=O species [18]. At the same time these positions represent potential anchoring sites for the cobalt. However, the characterization techniques (XRD, NH_3-chemisorption) have shown that all the cobalt is not anchored, therefore the above catalysts still exhibit a high acidity.

H_2-chemisorption measurements indicate two main features of these catalysts: firstly, small reduction degrees of cobalt, and secondly, a rather high metal dispersion for such a high metal content. Actually both features account for the same characteristic of these catalysts, namely the high homogeneity of the materials.

We have no clear proof for the existence of a SMSI effect. In a previous study [14] concerning Co–Nb_2O_5 catalysts we have identified several types of niobia in several oxidation states. A similar effect was reported by Brown and Kemball [19] for Pt–Nb_2O_5 and Rh–Nb_2O_5 catalysts. In this case Nb_2O_5 and $CoNb_2O_6$ were detected and it is difficult to speculate on such effect.

The experimental results in hydrogenolysis of butane confirms the fact that the crystallite size of the metal is a key factor in this reaction [20]. One can thus explain the low reaction rates we have determined. We fully agree with the model of Frydman et al. [21] who suggested that the surface of the support is covered by a homogeneous layer of Co^{2+} and islands of reduced Co. However, the diameter of these islands is unusually small for such a high concentration.

In a previous study we have suggested that the support is not inert at all [11]. In this study it was found that indeed 15 wt.% niobia causes an increase of the acidity and we suggest that this increase of acidity as well as the high metal dispersion leads to an increased life time of the catalysts. For the same experimental conditions and the same content of Co, the conversion on Co–Nb_2O_5–SiO_2 after 30 min is about 20% higher than the conversion on Co–Nb_2O_5 catalysts. Very recently, Fujimoto and Nakamura [22] suggested that it is likely that dehydrogenated species spill over on the support. Small metal particles should facilitate such a behavior leading to a clean metal surface. In such a way one can also interpret the higher isobutane selectivity as compared with results on Co–Nb_2O_5.

5. Conclusions

The preparation of Co–Nb_2O_5–SiO_2 catalysts using various sol–gel procedures leads to complex solids. No mixed niobium or cobalt compounds with silicon were found. A cobalt niobate phase was identified. The resulting catalysts contain a support matrix with acid properties and highly dispersed reduced cobalt.

The behavior of these catalysts in hydrogenolysis of butane account for these properties. The low reaction rates are assigned to the effect of the metal size, whereas the selectivity to isobutane and the relatively high stability are assigned to the acidity of the support.

References

[1] K. Tanabe, CHEMTECH 21 (1991) 628.
[2] D.A.G. Aranda, A.L.D. Ramos, F.B. Passos, M. Schmal, Catal. Today 28 (1996) 105.
[3] E.I. Ko, S.M. Maurer, J. Chem. Soc., Chem. Commun. (1990) 1062.
[4] S.M. Maurer, E.I. Ko, J. Catal. 135 (1992) 125.
[5] I. Iibrahim, N.F.A. Bright, J. Am. Ceram. Soc. 45 (1962) 221.
[6] K. Tanabe, M. Misono, Y. Ono, H. Hattori, Studies on Surface Science and Catalysis, Vol. 51, Elsevier, Amsterdam, 1989, p. 32.
[7] M. Shirai, N. Ichikumi, K. Asakura, Y. Iwasawa, Catal. Today 8 (1990) 57.
[8] P.A. Burke, E.I. Ko, J. Catal. 129 (1991) 38.
[9] J. Datka, A.M. Turek, J.M. Jehng, I.E. Wachs, J. Catal. 135 (1992) 186.
[10] S.M. Maurer, D. Ng, E.I. Ko, Catal. Today 16 (1993) 319.
[11] V. Pârvulescu, M. Ruwet, P. Grange, V.I. Pârvulescu, J. Mol. Catal. A 135 (1998) 75.
[12] R.C. Reuel, C.H. Bartholomew, J. Catal. 35 (1984) 63.
[13] G.C. Bond, J.C. Slaa, J. Mol. Catal. A 101 (1995) 243.
[14] G.C. Bond, J.C. Slaa, J. Mol. Catal. A 106 (1996) 135.
[15] G.C. Bond, Chem. Soc. Rev. 20 (1991) 441.
[16] B. Coq, E. Crabb, M. Warawdekar, G.C. Bond, J.C. Slaa, S. Galvagno, L. Mercadante, J.G. Ruiz, M.C.S. Sierra, J. Mol. Catal. 92 (1994) 107.
[17] F.B. Passos, M. Schmal, M.A. Vannice, J. Catal. 160 (1996) 106.
[18] J.-M. Jehng, I.E. Wachs, Catal. Today 16 (1993) 417.
[19] R. Brown, Ch. Kemball, J. Chem. Soc., Faraday Trans. 92 (1996) 281.
[20] V. Ponec, G.C. Bond, Catalysis by metals and alloy, Studies on Surface Science and Catalysis, Vol. 95, Elsevier, Amsterdam, 1995, p. 284.
[21] A. Frydman, D.G. Castner, M. Schmal, C.T. Cambell, J. Catal. 152 (1995) 164.
[22] K. Fujimoto, I. Nakamura, Studies on Surface Science and Catalysis, Vol. 112, Elsevier, Amsterdam, 1997, p. 29.